Inter-relationship between sphingosine kinase and phospholipase D in signaling *Arabidopsis* response to abscisic acid

Liang Guo, Girish Mishra, Jonathan E. Markham, Maoyin Li, Amanda Tawfall, Ruth Welti and Xuemin Wang

Published Version Information

Citation: Guo, L., Mishra, G., Markham, J. E., Li, M., Tawfall, A., Welti, R., & Wang, X. (2012). Connections between sphingosine kinase and phospholipase D in the abscisic acid signaling pathway in *Arabidopsis*. Journal of Biological Chemistry, 287(11), 8286-8296.

Digital Object Identifier (DOI): doi:10.1074/jbc.M111.274274

Publisher's Link: http://www.jbc.org/content/287/11/8286.full

Inter-relationship between Sphingosine Kinase and Phospholipase D in Signaling *Arabidopsis* Response to Abscisic Acid

Liang Guo[a,b], Girish Mishra[a,b, 1], Jonathan E. Markham[b, 2], Maoyin Li[a,b], Amanda Tawfall[a,b], Ruth Welti[c] and Xuemin Wang[a,b]

[a]*Department of Biology, University of Missouri, St. Louis, MO 63121,* [b]*Donald Danforth Plant Science Center, St. Louis, MO 63132, and* [c]*Kansas Lipidomics Research Center, Division of Biology, Kansas State University, Manhattan, KS 66506*

Address correspondence to: Xuemin Wang, Department of Biology, University of Missouri, St. Louis, MO 63121. Tel. 314-516-6219; Fax 314-587-1519; E-mail: wangxue@umsl.edu

Phosphatidic acid (PA) and phytosphingosine-1-phosphate (phyto-S1P) both are lipid messengers involved in plant response to abscisic acid (ABA). Our previous data indicate that PA binds to sphingosine kinase (SPHK) and increases its phyto-S1P-producing activity. To understand the cellular and physiological functions of the PA-SPHK interaction, we isolated *Arabidopsis thaliana* SPHK mutants *sphk1-1* and *sphk2-1* and characterized them, along with *phospholipase Dα1* knockout, *pldα1,* in plant response to ABA. Compared to wild-type (WT) plants, the *SPHK* mutants and *pldα1* all displayed decreased sensitivity to ABA-promoted stomatal closure. Phyto-S1P promoted stomatal closure in *sphk1-1* and *sphk2-1*, but not in *pldα1*, whereas PA promoted stomatal closure in *sphk1-1, sphk2-1*, and *pldα1.* The ABA activation of PLDα1 in leaves and protoplasts was attenuated in the *SPHK* mutants, and the ABA activation of SPHK was reduced in *pldα1.* In response to ABA, the accumulation of long-chain base phosphate (LCBP) was decreased in *pldα1* whereas PA production was decreased in *SPHK* mutants, compared WT. Collectively, these results indicate that SPHK and PLDα1 act together in ABA response and that SPHK and phyto-S1P act upstream of PLDα1 and PA in mediating the ABA response. Whereas SPHKs are involved in the activation of PLDα1, the activity of PLDα1 further enhances SPHK activation via PA binding SPHKs. The data suggest that SPHK/phyto-S1P and PLDa1/PA are co-dependent in amplification of response to ABA, mediating stomatal closure in *Arabidopsis*.

Phosphatidic acids (PA) produced by phospholipase Ds (PLDs) have been identified as important lipid signaling molecules in cell growth, development, and stress responses in both plants and animals (1, 2). In *Arabidopsis*, the level of PAs increases rapidly under various conditions, including chilling, freezing, wounding, pathogen elicitation, dehydration, salt, nutrient starvation, nodule induction, and oxidative stress (1, 2, 3, 4). PLD and PAs are involved in the response of guard cells to abscisic acid (ABA) (5, 6, 7, 8). ABA failed to induce stomatal closure in *PLDα1*-deficient plants, whereas overexpression of *PLDα1* resulted in increased sensitivity to ABA (8). PLDα1 mediates ABA signaling via PA interacting with ABI1 phosphatase 2C (7). This interaction impedes the negative function of ABI1 in ABA response and mediates ABA-promoted stomatal closure (7, 9). On the other hand, PLDα1 interacts with the GDP-bound Gα to regulate stomatal opening (9). PLDα1 has also been implicated in ROS production in *Arabidopsis* through the regulation of NADPH oxidase activity to promote stomatal

closure (8). These studies indicate that PA is an important second messenger in the regulation of multiple mediators that determine stomatal aperture in response to ABA.

ABA is an important endogenous phytohormone regulating developmental processes and stress responses in plants (10, 11). In response to drought stress, ABA level increases rapidly and initiates a network of signaling pathways in guard cell leading to stomatal closure (11). In the past decade, considerable progress has been made toward understanding ABA signaling pathway, from perception to downstream signaling (12, 13). A number of intermediate components of ABA signaling pathway have been identified by forward and reverse genetic approaches (10, 11, 14). One advance in understanding ABA perception is the recent identification, by independent groups, of proteins, known as pyrabactin resistance 1 (PYR1), pyr1-like proteins (PYLs), or Regulatory Components of ABA Receptor (RCARs), as ABA receptors (15, 16, 17, 18). The proteins known as PYR, PYLs, or RCARs are soluble and exist in the cytosol and nucleus (17). A core signal transduction model has been proposed to describe the early steps in the ABA signaling pathway (15, 16). In response to stimuli, ABA binds to the receptor PYR/PYL/RCARs, resulting in inhibition of negative regulator type 2C protein phosphatases such as ABI1, allowing SNF1-related kinase 2 (SnRK2) activation, mediating downstream signaling (11). Other ABA receptors have been reported in *Arabidopsis* including Mg-chelatase (CHLH/GUN5) and G-protein-coupled receptors (GCR2, GTG1/2) (19, 20, 21). CHLH/GUN5 is located in the plastid while GCR2 and GTG1/2 are localized on the plasma membrane (19, 20, 21). Multiple ABA receptors in different cell locations suggest that multiple ABA perception sites may be involved in multiple ABA signaling pathways during plant development and stress responses (22).

Sphingolipids are essential components of eukaryotic membranes and their metabolites also function as important regulators of many cellular processes, including stomatal response to ABA (23, 24). Phosphorylated sphingolipids, such as sphingosine-1-phosphate (S1P), are potent messengers in the regulation of a variety of processes in animals, including cell proliferation and survival (25). A number of genes involved in sphingolipid biosynthesis have been identified and characterized in *Arabidopsis* (26, 27). These studies indicate important roles for sphingolipids in plant growth, development, and response to stresses. Phosphorylated long-chain bases (LCBP), such as S1P and phytosphingosine-1-phosphate (phyto-S1P), have been implicated in the regulation of ABA-mediated stomatal behavior through G proteins in plants (28, 29, 30, 31). A recent study suggests that sphingosine and S1P are absent in *Arabidopsis* leaves due to the lack of expression of sphingolipid Δ4-desaturase (32). However, plants have other LCBPs, including phyto-S1P, a LCBP produced by sphingosine kinase (SPHK) (30). Phyto-S1P is implicated as a signaling molecule regulating ABA-dependent stomatal movement (30).

SPHK activity was recently established in *Arabidopsis*, and two genes *SPHK1* (At4g21540) and *SPHK2* (At4g21534) have been cloned and characterized (30, 31, 33). Both SPHKs were active and able to use various long-chain bases (LCBs) as substrates (31, 33). SPHK activity was shown to be rapidly induced by ABA and the production of phyto-S1P was involved in promotion of stomatal closure in response to ABA (29, 30). Overexpression of *SPHK1* increased ABA sensitivity during stomatal closure and germination (31). However, the physiological function of SPHK2 is unknown, and the mode of regulation of SPHK activation remains elusive. We recently showed that PA interacted with SPHK1 and SPHK2 and promoted their activity *in vitro* (33). This study

was undertaken to determine the cellular and physiological functions of the PA-SPHK interaction. The results show that PA interacts directly with SPHK in *Arabidopsis* and that PLDα1 and PA act downstream of SPHK. Together, PLDα1/PA and SPHK/phyto-S1P function in a positive feedback loop to amplify the ABA signal for stomatal closure in *Arabidopsis.*

EXPERIMENTAL PROCEDURES

Knockout Mutant Isolation and Complementation - *Arabidopsis thaliana* (Col-0) wild type (WT) and two T-DNA mutant (Salk_000250 and Salk_042034) lines were obtained from ABRC at Ohio State University. A PCR-based approach was used to verify the insertion of T-DNA and the homozygous T-DNA lines. T-DNA left border primer (LBa1) is 5`-TGGTTCACGTAGTGGGCCATCG-3`. Gene specific primers for Salk_000250 are 5`-CAGATTCCTCCTGCCTCTTTC-3` (RP2) and 5`-GGGAGCTAGAGGATTTGAAGG-3` (LP2). Gene specific primers for Salk_042034 are 5`-ATTCCCTTGTGGTTGTGTGTG-3` (RP1) and 5`-AACGGATTCACAAACACAAGC-3` (LP1). *pldα1* (Salk_053785) was isolated and confirmed previously (7). *PLDα1* and *SPHK* double mutants were generated by crossing *pldα1* with Salk_000250 and Salk_042034. To complement the SPHK mutants, genomic sequence including both *SPHK1* and *SPHK2* was cloned using two primers (5`-AGCCTTTTGGGTGGTGCACG-3` and 5`-AGCTAAACAAAATACTCTCTG-3`) and inserted into binary vector PEC291 for transformations of the SPHK mutants.

Plant Growth Conditions and Treatments - Plants were grown in soil in a growth chamber with cool white light of 160 µmol m^{-2} s^{-1} under 12 h light/ 12 h dark and 23°C/19°C cycles. The seed germination assay and root elongation assay were performed on agar plates containing ½ Murashige and Skoog (MS) medium supplemented with 1% sucrose. Desiccated seeds were sterilized in 70% ethanol followed by 20% bleach, rinsed three times with sterilized water, and placed on plates with or without ABA. The plates were kept at 4°C for 2 days before moving to the growth chamber under the same conditions described previously. For root elongation measurements, 4 day-old seedlings were transferred to ½ MS medium with 0 to 10 µM ABA; root lengths were recorded daily.

RNA Extraction and Real-time PCR - Real-time PCR was performed as described previously (34). Briefly, total RNA was digested with RNase-free DNase I and 1 µg RNA was used for synthesis of the first-strand cDNA using an iScript cDNA synthesis kit in a total reaction volume of 20 µL according to the manufacturer's instructions (Bio-Rad). The primer sequences were described previously (33). The efficiency of the cDNA synthesis was assessed by real-time PCR amplification of a control gene encoding UBQ10 (At4g05320). cDNAs were then diluted to yield similar threshold cycle (Ct) values based on the Ct of the *UBQ10*. The level of individual gene expression was normalized to that of *UBQ10* by subtracting the Ct value of UBQ10 from the tested genes. PCR was performed with a MyiQ system (Bio-Rad) using SYBR Green. Each reaction contained 7.5 µL 2×SYBR Green master mix reagent (Bio-Rad), 3.5 µL diluted cDNA, and 200 nM of each gene-specific primer in a final volume of 15 µL. The following standard thermal profile was used for all PCRs: 95°C for 3 min; and 50 cycles of 95°C for 30s, 55°C for 30 s, and 72°C for 30 s.

Stomatal Aperture Measurements - Stomatal aperture was measured according to procedure described by Zhang *et al.* (7). In brief, epidermal peels were floated in incubation buffer (10 mM KCl, 0.2 mM $CaCl_2$, 0.1 mM EGTA, 10 mM Mes-KOH, pH 6.15) for 2.5 h under cool white

light at 23°C to induce stomatal opening. 25 µM ABA, 10 µM phyto-S1P, 10 µM phyto-S1P with 0.1% 1-butanol and 50 µM PA were applied separately. Epidermal peels were incubated for 2.5 h under cool white light at 23°C to induce stomatal closure. Stomata were imaged under a microscope with a digital camera and analyzed with ImageJ software (NIH).

Purification of SPHK from Protoplasts and Immunoprecipitation - Mesophyll protoplasts were isolated from 4 week-old *Arabidopsis* leaves overexpressing *SPHK1* according to a procedure previously described (35). Protoplast labeling and protein extraction was performed as described previously (7). Protoplasts were labeled with 0.5 mg/mL 1-palmitoyl-2-{12-[(7-nitro-2-1,3-benzoxadiazol-4-yl)amino]dodecanoyl}-*sn*-glycero-3-phosphocholine (NBD-PC, Avanti) for 80 min and washed two times with the protoplast W5 buffer (35) to remove unlabeled NBD-PC. NBD-PC-labeled protoplasts were treated with 50 µM ABA for 30 min, followed by lysis in protoplast lysis buffer (20 mM Tris-HCl pH 7.5, 20 mM KCl, 1 mM EDTA, 10 mM DTT, 0.5% Triton X-100, 50% glycerol, 10 g/mL antipain, 10 g/mL leupeptin, 10 g/mL pepstatin, 1 mM phenylmethylsulfonyl fluoride) on ice for 5 min. Spermidine (5 mM) was added to the lysate followed by centrifugation at 10,000 *g* for 10 min. The cellular extract was incubated with ANTI-FLAG beads (Sigma) at 4°C for 3 h. The beads were pelleted by centrifugation and washed three times. Washed beads were extracted with chloroform:methanol:water (2:1). The extracts were dried under a stream of N_2, dissolved in chloroform, and separated by TLC (silica gel 60 F254; Merck, Darmstadt, Germany). NBD-PA, scraped from TLC plates, was quantified using a fluorescence spectrophotometer, by comparing fluorescence intensities to those on a standard curve constructed with known amounts of NBD-PA.

Fluorescence-based In Vivo Assay of Sphingosine Kinase Activity - Protoplasts were prepared from fully expanded leaves of 4 week-old *Arabidopsis*. Protoplasts were incubated in 0.1 mg/mL NBD-sphingosine for 80 min on ice and washed briefly. Washed protoplasts were kept at room temperature for 30 min. To determine *in vivo* sphingosine kinase activity based on the production of NBD-sphingosine-1-phosphate (NBD-S1P), 100 µM ABA was added to NBD-sphingosine-labeled protoplasts (~3×10^5) and incubated in a glass tube at room temperature for the indicated time (0-20 min). 800 µL chloroform:methanol:concentrated HCl (100:200:1; v/v/v) was added to extract the lipids. 250 µL chloroform and 250 µL 2 M KCl were added sequentially. The sample was vortexed and centrifuged to generate a two-phase system. The lower chloroform phase was collected into a clean glass tube. Samples were dried under nitrogen and then resuspended in 50 µL chloroform. Lipid samples were spotted onto TLC plates and separated with chloroform:acetone:methanol:acetic acid:water (10:4:3:2:1; v/v/v/v). Lipids were visualized under UV illumination. The regions corresponding to NBD-S1P and NBD-sphingosine were marked, scraped from the plates, placed in 600 µL chloroform:methanol:water (5:5:1), vortexed, and centrifuged for 5 min at 15,000 g. The fluorescence (excitation 460 nm, emission 534 nm) of the eluted lipids was measured in a fluorescence spectrophotometer.

To assay the activity of the purified SPHK1 and SPHK2 using NBD-sphingosine as substrate, 1-10 µg NBD-sphingosine was incubated in sphingosine kinase buffer (20 mM Tris PH 7.4, 20% glycerol, 1 mM mercaptoethanol, 1 mM EDTA and 0.25% (v/v) Triton X-100, 1 mM ATP and 10 mM $MgCl_2$) with 10 µg SPHK1 or SPHK2 purified from *E. coli* for 10 min at 37°C. Lipid extraction and separation by TLC was described above.

Fluorescence-based In Vivo Assay of Phospholipase D Activity – A PLD activity assay was performed according to a procedure described previously (7). Protoplasts prepared from leaves of 4 week-old plants were incubated in 0.5 mg/mL NBD-PC for 80 min on ice. To determine PLD activity, as affected by ABA treatment at different time points *in vivo*, 100 µM ABA was added to the NBD-PC-labeled protoplasts, and 100 µL aliquots (~3×10^5) were transferred to a new tube at the end of each treatment. 0.4 mL hot isopropanol (75°C) was added, and the mixture incubated for 10 min at 75°C to inactivate PLD. Lipids were extracted with 0.5 mL chloroform:methanol:water (5:5:1). The phases were separated and 100 µL chloroform were added to the aqueous phase, vortexed, centrifuged at 15,000 g for 2 min, and the lower chloroform phases were pooled. Each sample was dried under a nitrogen and 20 µL chloroform:methanol (95:5) were added. NBD-PC and NBD-PA were separated by TLC developed in chloroform:methanol:NH_4OH (65:35:5) and visualized under UV illumination. The regions corresponding to NBD-PC and NBD-PA were marked and scraped from the plates. The scraped silica gel was placed in 600 µL chloroform:methanol (2:1), vortexed, and centrifuged for 5 min at 15,000 g. The eluted lipids were quantified by fluorescence spectrophotometry (excitation 460 nm, emission 534 nm).

ESI-MS/MS Analysis of Lipid Molecular Species - Lipids were extracted and PA analyzed by electrospray ionization tandem mass spectrometry (ESI-MS/MS) as described by Xiao *et al.* (36). Expanded leaves of 4 to 5 week-old plants were sprayed with 100 µM ABA with 0.01% Triton X-100. The leaves were excised and immersed in 3 mL of isopropanol with 0.01% butylated hydroxytoluene (preheated to 75°C) immediately after sampling. The experiment was repeated 3 times with 5 replicates of each treatment each time.

HPLC/ESI-MS/MS Analysis of LCBPs - Sample preparation and analysis of LCB(P)s was carried out according to the method described by Markham *et al.* with some modifications (37). Briefly, 4 to 5 week-old plants were sprayed with 100 µM ABA with 0.01% Triton X-100. The excised leaves were extracted 5 times with solvent H (lower phase of isopropanol/hexane/water, 55:20:25 (v/v/v)) with agitation in 60°C water bath for 15 min. The extract was transferred to a new glass tube and the combined extract was dried under a stream of nitrogen. Further steps of sample preparation and mass spectrometry analysis were carried out as described previously (37).

RESULTS

Manipulations of SPHKs and their Expression in Response to ABA - To determine the function of *SPHK1* and *SPHK2* in *Arabidopsis*, we isolated two T-DNA insertion mutant lines for *SPHK1* and *SPHK2*. *Sphk1-1* (Salk_042034) and *sphk2-1* (Salk_000250). Each has a T-DNA insertion before the gene (*SPHK1* or *SPHK2*) start codon (Figure 1A). Both lines were homozygous (Figure 1B). The mutant *sphk2* displayed almost no detectable *SPHK2* transcript, whereas its *SPHK1* expression level was comparable to WT, as quantified by real-time PCR. In *sphk1,* the *SPHK1* transcript was decreased by 81% compared to WT whereas the transcript of *SPHK2* was also somewhat lower than WT (Figure 1C). We genetically complemented *sphk1* and *sphk2* by introducing *SPHK1* and *SPHK2*, respectively, under the control of their native promoters. *SPHK2*-OE lines driven by 35S promoter were generated in our previous study (33).

SPHK activity was shown to be quickly induced by ABA in a previous study (29). To determine whether the transcript levels of *SPHK1* or *SPHK2* are increased in response to ABA, we sprayed WT *Arabidopsis* leaves with

ABA and checked the expression levels of *SPHK1* and *SPHK2* by real-time PCR. The transcript level of *ABI1* began to increase 5 min after ABA treatment, but the transcript level of *SPHK1* and *SPHK2* did not change significantly (Figure 1D). The results suggest that *SPHK1* and *SPHK2* are not induced at the transcriptional level by ABA (Figure 1D).

PA Interacts with SPHK and Promotes the Activity of SPHK in Arabidopsis - Our previous study using *E. coli*-expressed proteins showed that PA bound to SPHK1 and SPHK2, and the interaction promoted the SPHK activity *in vitro* (33). To demonstrate their interaction and function in plants, we isolated protoplasts from the *SPHK1*-OE line which expressed FLAG-tagged SPHK1. NBD-PC-labeled protoplasts were washed and treated with 50 μM ABA followed by lysis and immunoprecipitation with ANTI-FLAG beads. The lipid was extracted from the immunoprecipitated fraction and separated by TLC. NBD-PA was co-precipitated with SPHK1 (Figure 2A, inset). ABA treatment for 30 min increased the amount of NBD-PA pulled down with SPHK1 approximately 4 fold, suggesting that ABA activated PLDα1 and increased the amount of PA interacting with SPHK1 in *Arabidopsis* cells (Figure 2A).

To determine whether PA promotes SPHK activity in the cell, we developed an assay, using NBD-sphingosine-labeled protoplasts, for production of NBD-S1P *in vivo*. First, we used SPHK purified from *E. coli* to confirm that *Arabidopsis* SPHK could phosphorylate NBD-sphingosine. Both SPHK1 and SPHK2 phosphorylated NBD-sphingosine to NBD-S1P (Figure 2B). We then labeled protoplasts with NBD-sphingosine followed by treatment with ABA or PA. Lipid extracts were separated by TLC and photographed under UV light (Supplemental Figure 1). ABA treatment increased SPHK activity; the highest level of NBD-S1P was produced after 2.5 min of ABA treatment (Figure 2C). The level of NBD-S1P in *SPHK2*-OE protoplasts was 36% higher, whereas the level in *sphk1-1* and *sphk2-1* protoplasts was, respectively, 19% and 40% lower than WT at 2.5 min of ABA treatment (Figure 2C). The ABA-induced activity of SPHK was also impaired in *pldα1*; the level of NBD-S1P produced in *pldα1* was approximately 33% lower than that in WT. The results indicate that PLDα1 is involved in activating SPHK in response to ABA (Figure 2C).

To determine if the PLD product PA could stimulate SPHK in the cell, we added PA (18:1/18:1) to the protoplasts. Addition of PA increased NBD-S1P production by more than 60% in protoplasts of WT and *pldα1* at 5 min after treatment (Figure 2D). Similar to the ABA treatment, the increased SPHK activity in the PA treatment was the highest in *SPHK2*-OE and lower in *sphk1-1* and *sphk2-1* protoplasts. However, unlike the ABA treatment, PA-treated WT and *pldα1-1* protoplasts exhibited the same magnitude and pattern of NBD-S1P increase (Figure 2D). These data support the conclusion that SPHK is a target of PA and PLD-produced PA is involved in the SPHK activation in response to ABA.

SPHK Acts Upstream of PLDα1 in the Signaling Pathway of the ABA-mediated Stomatal Closure - To determine the relationship of SPHK/phyto-S1P and PLDα1/PA in the ABA signaling pathway, we measured stomatal aperture in response to phyto-S1P in *SPHK* and *PLDα1* mutants. Phyto-S1P produced by SPHK was shown previously to induce stomatal closure (30). We used phyto-S1P to treat epidermal peels and found that phyto-S1P caused stomatal closure in WT, *sphk1-1* and *sphk2-1* but not in *pldα1* or the double knockout mutants of *pldα1sphk1-1* or *pldα1sphk2-1* (Figure 3A). The result suggests that SPHK and phyto-S1P act upstream of PLDα1 and PA.

We then treated the epidermal peels with PA to determine the effect of PA on stomatal closure in these mutant lines. PA (18:1/18:1) was able to cause stomatal closure in WT, *pldα1*, *sphk1-1* and *sphk2-1* (Figure 3B). This result is consistent with the finding (Figure 3A) that PLDα1 and PA act downstream of SPHKs to promote stomatal closure. To augment the finding, we added 1-butanol, which decreases PA production by PLD, to the *Arabidopsis* epidermal peels treated with phyto-S1P. 1-Butanol partially blocked the phyto-S1P-promoted stomatal closure in WT, *sphk1-1,* and *sphk2-1*, but had no effect on *pldα1* (Figure 3A). The results support the notion that PLD/PA is involved in mediating phyto-S1P signal in stomatal closure.

ABA-Promoted PLDα1 Activation Is Attenuated in SPHK Mutants - The above results indicate that both SPHK and PLDα1 are involved in the same signaling pathway in ABA-promoted stomatal closure, with SPHK and phyto-S1P acting upstream of PLDα1. To define the effect of SPHK on PLD activity and PA production in response to ABA, we measured PA production *in vivo* using NBD-PC-labeled leaf protoplasts exposed to ABA or phyto-S1P. The production of PA increased almost two fold in WT in 40 min after the start of ABA treatment (Figure 4A, 4B). However, the increase in PA in both *sphk1-1* and *sphk2-1* was significantly smaller than that in WT. Compared to WT, after 40 min of ABA treatment, PA production in *sphk1-1* and *sphk2-1* was 17% and 30% lower, respectively (Figure 4B). In *pldα1,* the PA level was lower than WT and *SPHK* mutants, and there was no significant increase in PA (Figure 4B), supporting the previous conclusion that PLDα1 is the major PLD responsible for ABA-induced PA production (7).

We reasoned that if PLDα1 acts downstream of SPHK, phyto-S1P should be able to activate PLDα1. To test this hypothesis, we first tested whether phyto-S1P could stimulate PLDα1 directly *in vitro.* Additions of different concentrations of phyto-S1P failed to increase PLDα1 directly, indicating other cellular effectors are involved in the PLD activation by phyto-S1P (Supplemental Figure 2). We then treated the protoplasts with phyto-S1P and measured PA production in protoplasts (Figure 4C). The production of PA was increased by approximately two fold by phyto-S1P in WT and both *SPHK* mutants. PA reached the highest level after 10 min of incubation. Knockout of *PLDα1* abolished the ABA or phyto-S1P-induced increase in PA (Figure 4B, 4C). The response of PLD activity to phyto-S1P indicates that SPHK and phyto-S1P are involved in activation of PLDα1 to produce PA in response to ABA.

ABA Induces Different PA Changes in WT, sphk1-1, sphk2-1 and SPHK2-OE Lines - To characterize the effect of SPHKs on PA production in response to ABA, we quantitatively profiled the changes in PA species in *Arabidopsis* leaves sprayed with ABA using ESI-MS/MS. Knockout of PLDα1 reduced the PA production in response to ABA (8). The total amount of PA in *sphk1-1* and *sphk2-1* was not significantly different than that of WT without ABA treatment (Figure 5A). In WT, PA reached the highest level at 10 min after ABA treatment and then went down to the pretreatment level after 40 min (Figure 5A). The total PA level was also increased in *sphk1-1*, *sphk2-1,* and *SPHK2*-OE leaves after ABA treatment (Figure 5A). The PA level was higher than WT after ABA treatment in *SPHK2*-OE. However, the amount of PA was significantly lower in *sphk1-1* and *sphk2-1* treated by ABA for 5 and 10 min than in WT (Figure 5A). The results indicate that decreased SPHK expression attenuates ABA-induced activation of PLDα1, in agreement with the results for the *in vivo* PLD activity assay (Figure 4B).

The change of PA species in response to ABA at 10 min was analyzed for WT, *pldα1*, *sphk1-1, sphk2-1* and *SPHK2*-OE. The major PAs in WT *Arabidopsis* leaves are 34:2 (16:0/18:2), 34:3 (16:0/18:3), 36:4 (mainly 18:2/18:2), 36:5 (18:2/18:3), and 36:6 (18:3/18:3) (8, 38). The levels of all PA species were decreased in *pldα1* and the major overall decreases were due to decreases in 34:2 PA and 34:3 PA, two very abundant PAs in *Arabidopsis* leaves (Figure 5B). In comparison, the levels of most PA species (except 36:6 and 36:5 PA) were higher in WT than in *sphk1-1* and *sphk2-1* after 10 min of ABA treatment (Figure 5B). Overexpression of *SPHK2* mainly resulted in higher levels of 34:2 PA and 34:3 PA compared to WT and other PA species did not change significantly (Figure 5B). The results show that the activation of *SPHK1* and *SPHK2* affects levels of 34-carbon PAs more than other PAs.

LCBP Profiling Reveals Regulation of SPHK by PA - To determine the effect of PLDα1/PA on the level of different LCBPs in *Arabidopsis*, LCBP species were profiled to measure LCBP changes in response to ABA. We first analyzed the LCBPs in *Arabidopsis* leaves from WT and mutant lines. The total content of four major LCBP species (d18:0-P, d18:1-P, t18:0-P and t18:1-P) was comparable in WT, *pldα1,* and *sphk1-1* (Figure 6A). The LCBP level in *sphk2-1* was about 57% lower than that in WT, indicating that ablation of *SPHK2* dramatically decreased LCBP production in *Arabidopsis* leaves (Figure 6A). Total LCBP level was increased by 40% when *SPHK2* was overexpressed in *Arabidopsis* (Figure 6A). The lower level of total LCBP in *sphk2-1* was mainly due to the decrease of t18:0-P and t18:1-P (Figure 6B). ABA treatment increased the LCBP content by 58% in WT leaves at 2 min after ABA treatment. Knockout of *PLDα1* or either *SPHK* gene resulted in a reduction of LCBP levels after ABA treatment (Figure 6C).

LCBP species displayed different patterns of changes in response to ABA treatment (Figure 6D). The increase in t18:0-P is transitory and occurred early, peaking at 2 min after treatment. The increase in d18:1-P peaked at 5 min whereas d18:0-P increased steadily over the 15 min tested. The mutant *sphk1* displayed transitory changes similar to WT, except that the magnitude of increase was smaller. However, *sphk2* did not exhibit the same level of transitory change in t18:0-P as WT, but d18:0-P and d18:1-P changed, peaking 5 min after treatment (Figure 6D). LCBP production in *pldα1* was not induced by ABA as much as in WT, indicating knockout of *PLDα1* reduced SPHK activation by ABA (Figure 6D). This indicates that PA is involved in SPHK activation in response to ABA.

SPHK2-KO and OE Alter Arabidopsis Sensitivity to ABA - To determine the effect of *SPHK1* and *SPHK2* mutations on *Arabidopsis* response to ABA, we assayed ABA responses of *sphk1-1* and *sphk2-1* together with *SPHK2*-OE lines. Stomatal aperture was decreased by ABA in WT. However, *sphk1-1* and *sphk2-1* were less sensitive to ABA-promoted stomatal closure (Figure 7A). Double mutants *pldα1sphk1-1* and *pldα1sphk2-1* were insensitive to ABA-caused stomatal closure like *pldα1* (Figure 7A). Introducing a genomic sequence containing both *SPHK1* and *SPHK2* under their native promoters into *sphk1-1* and *sphk2-1* restored the stomatal response to ABA for both mutants, indicating that loss of *SPHK1* and *SPHK2* is responsible for the ABA response phenotype (Figure 7A).

Knockdown of *SPHK1* or *SPHK2* decreased while overexpression of *SPHK2* increased ABA sensitivity during ABA-inhibited root elongation (Figure 7B). The root length of the two *SPHK* mutants was longer than that of WT under 5 μM or 10 μM ABA. Overexpression of *SPHK2* increased ABA sensitivity during ABA-inhibited root elongation as the root lengths in the OE lines were shorter than that of WT (Figure 7B).

Manipulation of *SPHK1* and *SPHK2* also altered ABA sensitivity during seed germination and post-germination growth. *Sphk1-1* and *sphk2-1* germinated earlier than WT on ½ MS plates with different concentrations of ABA whereas the germination of *SPHK2*-OE seeds was delayed and its postgermination growth was inhibited (Figure 7C, 7D). The data suggest that *SPHK2* is involved in the control of three ABA responses in *Arabidopsis*.

DISCUSSION

SPHK1 and *SPHK2* are two tandem repeat genes closely linked on chromosome 4 in *Arabidopsis* (33). We isolated two T-DNA mutants, *sphk1-1* and *sphk2-1*, for *SPHK1* and *SPHK2* separately. Real-time PCR indicated that *SPHK1* expression level was dramatically reduced in *sphk1-1* whereas the transcript of *SPHK1* was slightly induced in *sphk2-1*. This provides more evidence that *SPHK1* and *SPHK2* are two separate genes and have their own promoters. *SPHK1* was reported to have a role in two ABA signaling pathways in regulation of stomatal aperture and seed germination (31). The present study shows that both *SPHK* mutants display decreased sensitivity to ABA-promoted stomatal closure, ABA-inhibited root elongation and ABA-inhibited seed germination. In addition, *SPHK2*-OE lines were more sensitive to ABA in three ABA-mediated responses, indicating that *SPHK2* is involved in ABA-mediated signaling pathways.

Quantitative analysis of LCBP showed that the total LCBP level remained the same as WT in *sphk1-1* but decreased about 57% in *sphk2-1*. The decreased LCBP content mainly came from t18:0-P and t18:1-P. There was still 43% of LCBP in *sphk2-1* compared to WT, which is presumably a result of *SPHK1* and other kinases including AtLCBK1 and AtCERK (39, 40). These data indicate that whereas SPHK2 contributes more than SPHK1 to LCBP production in leaves, SPHK1 and SPHK2 have unique and overlapping functions in LCBP synthesis in *Arabidopsis* leaves. Availability of *SPHK1xSPHK2* double knockout mutants will be helpful to further determine the functions of both SPHKs. But isolating such mutants by crossing *sphk1-1* and *sphk2-1* has been unsuccessful because *SPHK1* and *SPHK2* are closely linked (33).

Our previous *in vitro* study showed that PA binds to SPHKs and stimulates their activity, suggesting that *Arabidopsis* SPHKs are molecular targets of PA (33). The present study using protoplasts provides *in vivo* evidence that PA binds to and stimulates SPHK. More evidence was garnered from the SPHK activity assay and quantitative profiling of LCBPs from leaves. Addition of PA promoted the production of NBD-S1P in WT protoplasts and SPHK activity was attenuated in *pldα1* when protoplasts were treated with ABA. LCBP analysis indicated that LCBP content increased by 58% in WT *Arabidopsis* leaves after a 2 min ABA treatment. Knockout of *PLDα1* resulted in less than 10% increase of LCBP in response to ABA treatment, indicating PLDα1 and PA were involved in promotion of SPHK activity in response to ABA.

Phyto-S1P (t18:0-P) was capable of promoting stomatal closure (30). Phyto-S1P is one of the major LCBPs found in *Arabidopsis* leaves; it can serve as a signaling molecule to mediate ABA response. Our data show that ABA induced the increased production of all 4 LCBPs in *Arabidopsis* leaves. Whether the other three LCBPs are involved in ABA-mediated signaling pathway needs to be determined. LCBPs have broad cellular functions in animals, and more functions of LCBPs in plants also should be explored.

The phenotypic analysis of stomata in this study also indicates that PLD/PA and SPHK/phyto-S1P are involved in the same pathway in regulation of stomatal closure. *pldα1*

was insensitive to phyto-S1P-promoted stomatal closure. PLD enzyme activity assay showed that phyto-S1P activated PLDα1 in *Arabidopsis* cells, placing PLDα1 downstream of SPHK in ABA signaling pathway. Lipid profiling also revealed that all the PA species were increased in response to ABA in WT leaves. Our previous study indicated that not all PA species interacted with SPHK and promoted its activity. Among the PA species tested, 16:0/16:0 PA, 18:1/18:1 PA, 16:0/18:1 PA and 16:0/18:2 PA were able to bind to both SPHK1 and SPHK2 (33). 18:1/18:1 (36:2), 16:0/18:1(34:1) and 16:0/18:2 (34:2) PA naturally exist in *Arabidopsis* leaves and their levels are induced by ABA treatment. PA can be produced by multiple enzymes in response to different stimuli (1). PA regulates multiple proteins mediating ABA signaling, including ABI1, NADPH oxidases, and SPHKs (7, 8, 33). Many other PA-interacting proteins such as PDK1, CTR1 and TGD2 have also been identified in plants (41, 42, 43). Available data suggest that regulation of different proteins by PA depends on PA species and sources, timing, and localization of PA production.

In summary, the present physiological, genetic, and enzymatic analyses combined with lipid profiling clearly indicate a co-dependency between the two lipid signaling reactions, SPHK/phyto-S1P and PLD/PA (Figure 8). PA produced by PLDα1 interacts with SPHK and is required for SPHK activation in response to ABA. Increased phyto-S1P activates PLDα1, leading to an increase in PA level. PA functions as a signaling molecule to regulate downstream proteins including ABI1 and NADPH oxidase in ABA-mediated stomatal closure. The ABA signal is transduced to downstream pathways and regulates ion channels, leading to stomatal closure (Figure 8). It will be of interest in future studies to determine whether the interplay between PLDα1/PA and SPHK/phyto-S1P is involved in other signaling and regulatory pathways in plant growth, development, and response to stresses.

REFERENCES

1. Wang, X., Devaiah, S. P., Zhang, W., and Welti, R. (2006) *Prog. Lipid Res.* **45**, 250-278
2. Bargmann, B. O., and Munnik, T. (2006) *Curr. Opin. Plant Biol.* **9**, 515-522
3. Li, M., Hong, Y., and Wang, X. (2009) *Biochim. Biophys. Acta* **1791**, 927-935
4. Hong, Y., Zheng, S., and Wang, X. (2008) *Molecular Plant* **1,** 262-269
5. Ritchie, S., and Gilroy, S. (1998) *Proc. Natl. Acad. Sci. U.S.A.* **95**, 2697-2702
6. Jacob, T., Ritchie, S., Assmann, S. M., and Gilroy, S. (1999) *Proc. Natl. Acad. Sci. U.S.A.* **96**, 12192-12197
7. Zhang, W., Qin, C., Zhao, J., and Wang, X. (2004) *Proc. Natl. Acad. Sci. U.S.A.* **101**, 9508-9513
8. Zhang, Y., Zhu, H., Zhang, Q., Li, M., Yan, M., Wang, R., Wang, L., Welti, R., Zhang, W., and Wang, X. (2009) *Plant Cell* **21**, 2357-2377
9. Mishra, G., Zhang, W., Deng, F., Zhao, J., and Wang, X. (2006) *Science* **312**, 264-266
10. Raghavendra, A. S., Gonugunta, V. K., Christmann, A., and Grill, E. (2010) *Trends Plant Sci.* **15**, 395-401
11. Hubbard, K. E., Nishimura, N., Hitomi, K., Getzoff, E. D., and Schroeder, J. I. (2010) *Genes Dev.* **24**, 1695-1708
12. Schroeder, J. I., Kwak, J. M., and Allen, G. J. (2001) *Nature* **410**, 327-330
13. Hirayama, T., and Shinozaki, K. (2007) *Trends Plant Sci.* **12**, 343-351
14. Pandey, S., Nelson, D. C., and Assmann, S. M. (2009) *Cell* **136**, 136-148

15. Park, S. Y., Fung, P., Nishimura, N., Jensen, D. R., Fujii, H., Zhao, Y., Lumba, S., Santiago, J., Rodrigues, A., Chow, T. F., Alfred, S. E., Bonetta, D., Finkelstein, R., Provart, N. J., Desveaux, D., Rodriguez, P. L., McCourt, P., Zhu, J. K., Schroeder, J. I., Volkman, B. F., and Cutler, S. R. (2009) *Science* **324**, 1068-1071
16. Ma, Y., Szostkiewicz, I., Korte, A., Moes, D., Yang, Y., Christmann, A., and Grill, E. (2009) *Science* **324**, 1064-1068
17. Nishimura, N., Sarkeshik, A., Nito, K., Park, S. Y., Wang, A., Carvalho, P. C., Lee, S., Caddell, D. F., Cutler, S. R., Chory, J., Yates, J. R., and Schroeder, J. I. (2009) *Plant J.* **61**, 290-299
18. Nishimura, N., Hitomi, K., Arvai, A. S., Rambo, R. P., Hitomi, C., Cutler, S. R., Schroeder, J. I., and Getzoff, E. D. (2009) *Science* **326**, 1373-1379
19. Shen, Y. Y., Wang, X. F., Wu, F. Q., Du, S. Y., Cao, Z., Shang, Y., Wang, X. L., Peng, C. C., Yu, X. C., Zhu, S. Y., Fan, R. C., Xu, Y. H., and Zhang, D. P. (2006) *Nature* **443**, 823-826
20. Liu, X., Yue, Y., Li, B., Nie, Y., Li, W., Wu, W. H., and Ma, L. (2007) *Science* **315**, 1712-1716
21. Pandey, S., Nelson, D. C., and Assmann, S. M. (2009) *Cell* **136**, 136-148
22. Umezawa, T., Nakashima, K., Miyakawa, T., Kuromori, T., Tanokura, M., Shinozaki, K., and Yamaguchi-Shinozaki, K. (2010) *Plant Cell Physiol.* **51**, 1821-1839
23. Lynch, D. V., Chen, M., and Cahoon, E. B. (2009) *Trends Plant Sci.* **14**, 463-466
24. Dunn, T. M., Lynch, D. V., Michaelson, L. V., and Napier, J. A. (2004) *Ann. Bot.* **93**, 483-497
25. Spiegel, S., and Milstien, S. (2003) *Nat. Rev. Mol. Cell Biol.* **4**, 397-407
26. Chen, M., Han, G., Dietrich, C. R., Dunn, T. M., and Cahoon, E. B. (2006) *Plant cell* **18**, 3576-3593
27. Chen, M., Markham, J. E., Dietrich, C. R., Jaworski, J. G., and Cahoon, E. B. (2008) *Plant cell* **20**, 1862-1878
28. Ng, C. K., Carr, K., McAinsh, M. R., Powell, B., and Hetherington, A. M. (2001) *Nature* **410**, 596-599
29. Coursol, S., Fan, L. M., Le Stunff, H., Spiegel, S., Gilroy, S., and Assmann, S. M. (2003) *Nature* **423**, 651-654
30. Coursol, S., Le Stunff, H., Lynch, D. V., Gilroy, S., Assmann, S. M., and Spiegel, S. (2005) *Plant Physiol.* **137**, 724-737
31. Worrall, D., Liang, Y. K., Alvarez, S., Holroyd, G. H., Spiegel, S., Panagopulos, M., Gray, J. E., and Hetherington, A. M. (2008) *Plant J.* **56**, 64-72
32. Michaelson, L. V., Zauner, S., Markham, J. E., Haslam, R. P., Desikan, R., Mugford, S., Albrecht, S., Warnecke, D., Sperling, P., Heinz, E., and Napier, J. A. (2009) *Plant Physiol.* **149**, 487-498
33. Guo, L., Mishra, G., Taylor, K., and Wang, X. (2011) *J. Biol. Chem.* **286**, 13336-13345
34. Li, M., Qin, C., Welti, R., and Wang, X. (2006) *Plant Physiol.* **140**, 761-770
35. Yoo, S. D., Cho, Y. H., and Sheen, J. (2007) *Nat. Protoc.* **2**, 1565-1572
36. Xiao, S., Gao, W., Chen, Q. F., Chan, S.W., Zheng, S.X., Ma, J., Wang, M., Welti, R., and Chye, M.L. (2010) *Plant Cell*, **22**, 1463-1482

37. Markham, J. E., and Jaworski, J. G. (2007) *Rapid Commun. Mass Spectrom.* **21**, 1304-1314
38. Devaiah, S. P., Roth, M. R., Baughman, E., Li, M., Tamura, P., Jeannotte, R., Welti, R., and Wang, X. (2006) *Phytochemistry* **67**, 1907-1924
39. Imai, H., and Nishiura, H. (2005) *Plant Cell Physiol.* **46**, 375-380
40. Liang, H., Yao, N., Song, J. T., Luo, S., Lu, H., and Greenberg, J. T. (2003) *Genes Dev.* **17**, 2636-2641
41. Anthony, R. G., Henriques, R., Helfer, A., Meszaros, T., Rios, G., Testerink, C., Munnik, T., Deak, M., Koncz, C., and Bogre, L. (2004) *Embo J.* **23**, 572-581
42. Testerink, C., Larsen, P. B., van der Does, D., van Himbergen, J. A., and Munnik, T. (2007) *J. Exp. Bot.* **58**, 3905-3914
43. Lu, B., and Benning, C. (2009) *J. Biol. Chem.* **284**, 17420-17427

FOOTNOTES

*This work was supported by the National Science Foundation Grant IOS-0818740 and the US Department of Agriculture Grant 2007-35318-18393. PA analyses were performed at the Kansas Lipidomics Research Center, where equipment acquisition and method development were funded by the National Science Foundation (EPS 0236913, MCB 0455318 and 0920663, DBI 0521587), Kansas Technology Enterprise Corporation, Kansas IDeA Network of Biomedical Research Excellence (K-INBRE) of National Institutes of Health (P20RR16475), and Kansas State University. The costs of publication of this article were defrayed in part by the payment of page charges. This article must therefore be hereby marked "*advertisement*" in accordance with 18 U.S.C. Section 1734 solely to indicate this fact.

[1]Present Address: Department of Botany, University of Delhi, New Delhi-110007, India
[2]Present Address: Department of Biochemistry, University of Nebraska, N146 Beadle Center, Lincoln, NE 68588

[3]***The abbreviations used are:*** ABA, abscisic acid; ABI1, ABA INSENSITIVE 1; PA, phosphatidic acid; PLD, phospholipase D; phyto-S1P, phytosphingosine-1-phosphate; SPHK, sphingosine kinase; LCB, long-chain base. LCBP, long-chain base phosphate.

Keywords: *Phosphatidic acid, phospholipase D, sphingosine kinase, stomatal closure,* ABA *signaling, lipid signaling*

FIGURE LEGENDS

FIGURE 1. Isolation of T-DNA insertion lines and expression of two *SPHK*s in *Arabidopsis* leaves. *A*, diagram showing the T-DNA insertion sites in Salk_042034 (*sphk1-1*) and Salk_000250 (*sphk2-1*). T-DNA is located in front of start codon of *SPHK1* and *SPHK2* separately. Thin lines represent non-coding regions and boxes represent exons. *B*, PCR genotyping of two T-DNA insertion lines. The presence of T-DNA band and lack of *SPHK1* or *SPHK2* band indicate that each is a homozygous T-DNA insertion mutant. PCR was

conducted using genomic DNA with a pair of gene specific primers (LP1+RP1 for *SPHK1* and LP2+RP2 for *SPHK2*) or a combination of T-DNA left border primer (LBa1) and gene specific primers (RP1 for *SPHK1* and RP2 for *SPHK2*). *C*, expression level of *SPHK1* and *SPHK2* in WT and T-DNA mutants determined by real-time PCR normalized to *UBQ10*. RNA was extracted from young leaves of 4 week-old *Arabidopsis*. The experiment was repeated three times. Values are means ± SE (n = 3) for one representative experiment. *D*, effect of ABA on *SPHK1* and *SPHK2* expression measured by real-time PCR normalized to *UBQ10*. The ABA response gene *ABI1* was used as a positive control. RNA was extracted from leaves sprayed with 100 μM ABA with 0.01% Triton X-100. The experiment was repeated three times. Values are means ± SE (n = 3) for one representative experiment.

FIGURE 2. PA interacts with SPHK and is involved in activation of SPHK in response to ABA. *A*, quantification of NBD-PA bound to SPHK1 pulled down by Anti-FLAG resin beads. Inset represents image of NBD-PA immunoprecipitated with SPHK1 on TLC plate. *B*, SPHK activity assay using NBD-sphingosine as substrate. NBD-S1P was produced by both SPHKs as indicated on TLC plate. *C*, quantification of NBD-S1P production in protoplasts treated with 50 μM ABA. Protoplasts were isolated from WT*, pldα1*, *sphk1-1, sphk2-1* and *SPHK2*-OE lines. D, quantification of NBD-S1P production in protoplasts treated with 50 μM PA. The level of NBD-S1P was calculated as the percentage of NBD-S1P over the total NBD-labeled lipids. Values in C and D are means ± SE (n = 3).

FIGURE 3. PLDα1 and PA mediate the phyto-S1P effecton the signaling pathway in ABA-mediated stomatal closure. *A*, effect of phyto-S1P on stomatal closure in WT and mutants. The epidermal peels were incubated in stomatal incubation buffe containing 10 μM phyto-S1P or 10 μM phyto-S1P plus 0.1% 1-butanol. Asterisks indicate that the mean value is significantly different from that of the samples treated with phyto-S1P at $P<0.05$ based on Student's *t* test. *B*, PA (18:1/18:1) induces stomatal closure in WT and mutants. Epidermal peels were treated with 50 μM PA. All values are means ± SE (n = 50) in the stomatal assays.

FIGURE 4. Activation of PLDα1 by ABA requires SPHK. *A*, representative image of fluorescent-based assay of PLD activity using NBD-PC-labeled protoplasts treated with 50 μM ABA. *B*, quantification of ABA-induced PA production in protoplasts isolated from WT*, pldα1*, *sphk1-1,* and *sphk2-1*. Protoplasts were labeled with NBD-PC followed by treatment with ABA. WT control was treated with 0.1% ethanol. *C*, quantification of phyto-S1P-promoted PA production in protoplasts isolated from WT*, pldα1*, *sphk1-1,* and *sphk2-1*. The level of PA was calculated as the percentage of NBD-PA over the total NBD-labeled lipids. Data in B and C are means ± SE (n = 3) for one representative experiment.

FIGURE 5. ABA-induced PA changes in *Arabidopsis* leaves. *A*, change in total PA content in leaves harvested at different times after spraying with ABA (100 μM). *B*, comparison of PA molecular species in leaves of WT*,* mutants, and *SPHK2*-OE lines treated with ABA for 10 min. The experiment was performed three times. Values in A and B are means ± SE (n = 5).

FIGURE 6. Alterations of SPHKs change LCBP content and composition in *Arabidopsis* leaves. *A*, total LCBP content (mol%) in leaves from 4 to 5 week-old WT, *pldα1*, *sphk1-1, sphk2-1,* and *SPHK2*-OE5. *B*, LCBP composition in leaves from 4 to 5 week-old WT, *pldα1*,

sphk1-1, sphk2-1, and *SPHK2*-OE5. *C,* total LCBP content in WT *Arabidopsis* leaves treated with ABA. 4 to 5 week-old *Arabidopsis* was sprayed with 100 μM ABA with 0.01% Triton X-100 followed by sphingolipid extraction and MS analysis. *D*, LCBP composition in the leaves treated with 50 μM ABA with 0.01% Triton X-100 for 0-15 min. Data were calculated as molar percentage over the total amount of LCB (sphinganine (d18:0), 8-sphingenine (d18:1), phytosphingosine (t18:0) and 4-hydroxy-8-sphingenine (t18:1)) and LCBP (d18:0-P, d18:1-P, t18:0-P and t18:1-P). The experiment was performed twice. Values are means ± SE (n = 5) for one experiment. Asterisks in B and C indicate that the mean value is significantly different from that of the WT at $P < 0.05$, based on Student's *t* test. Asterisks in D indicate that the mean value is significantly different from that of the 0 min ABA treatment at $P < 0.05$ based on Student's *t* test.

FIGURE 7. Altered ABA sensitivity in *SPHK-KO* mutants and *SPHK2* over-expression *Arabidopsis*. *A*, addition of ABA (25 μM) induced stomatal closure in WT and mutants lines. COM1 is a complimented line for *sphk1-1* and COM2 is a complimented line for *sphk2-1*. Values are means ± SE (n=50). Asterisks indicate that the mean value is significantly different from that of the WT treated with ABA at $P<0.05$ based on Student's *t* test. *B*, root growth of WT, *sphk1-1, sphk2-1,* and *SPHK2*-OE lines (OE2 and OE5) on ½ MS medium with 0 μM, 5 μM or 10 μM ABA. Values are means ± SE (n = 20) for one representative experiment. Asterisks indicate that the mean value is significantly different from that of the WT treated with same concentration of ABA at $P<0.05$ based on Student's *t* test. *C*, seed germination rate on ½ MS medium with different concentrations of ABA. Desiccated seeds were germinated on ½ MS with or without ABA and scored 3 days after transfer from 4℃. About 100 seeds per genotype were scored for each experiment. Values are means ± SE (n=3). *D*, seed germination and post-germination growth on ½ MS medium without ABA (left) or with 1 μM ABA at day 6.

FIGURE 8. Proposed model for the role of SPHK/phyto-S1P and PLDα1/PA in ABA-mediated stomatal closure signaling pathway. This model depicts only the known targets of PLD/PA in the ABA-mediated stomatal closure and other ABA regulators are not included in this model. ABA activates SPHKs through unknown mechanisms and ABA receptors may be involved. The activation of SPHKs produces phyto-S1P that activates PLDα1 to produce PA. PA inhibits ABI1 function but promotes NADPH oxidase to promote ABA-mediated stomatal closure. Meanwhile, PLDα1-produced PA stimulates SPHK activity through a positive feedback loop. Arrows with solid lines indicate established links and arrows with dashed lines denote putative links.

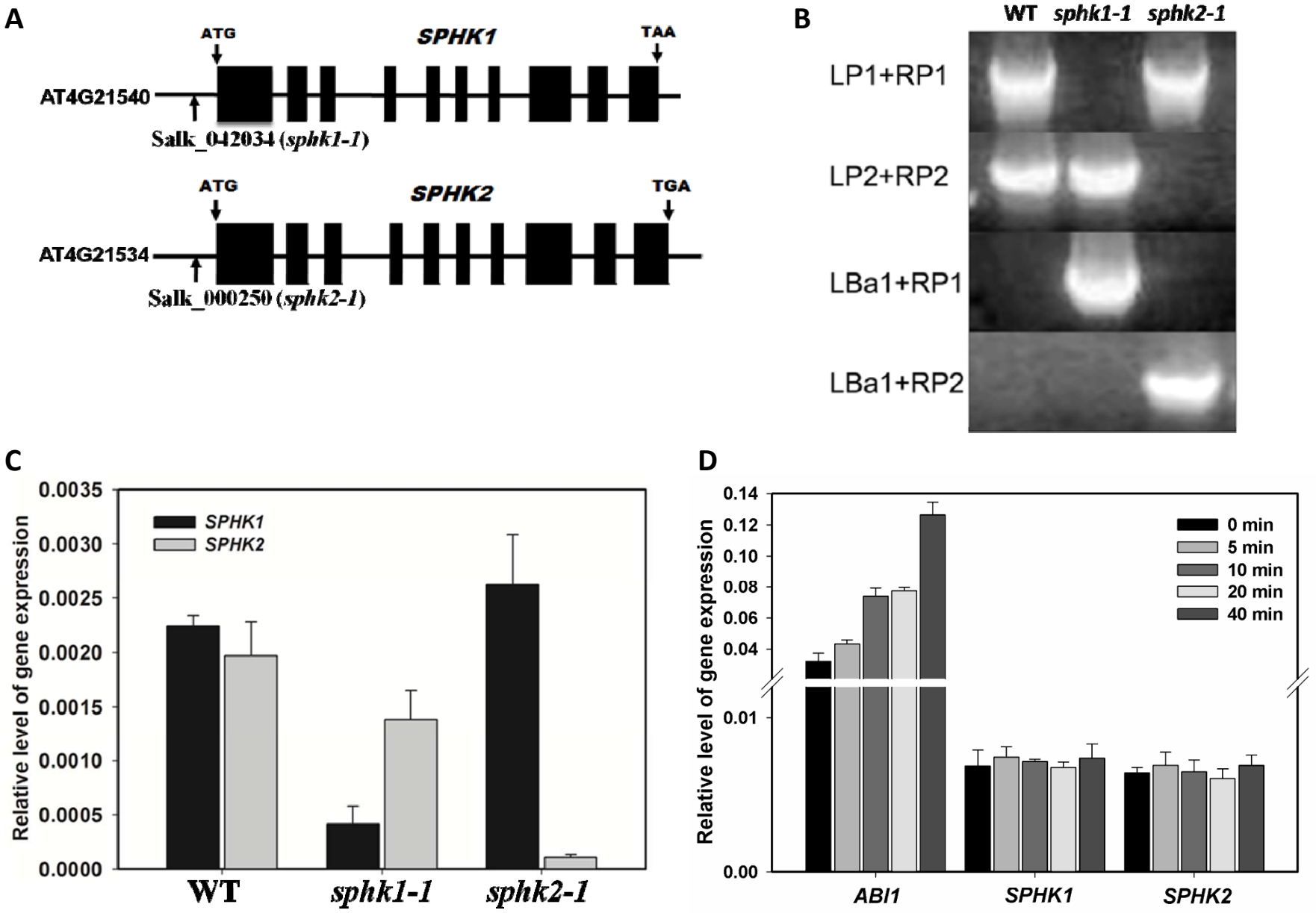
A
ATG
SPHK1
TAA
AT4G21540
Salk_042034 (sphk1-1)
ATG
SPHK2
TGA
AT4G21534
Salk_000250 (sphk2-1)
B
WT
sphk1-1
sphk2-1
LP1+RP1
LP2+RP2
LBa1+RP1
LBa1+RP2
C
Relative level of gene expression
0.0035
0.0030
0.0025
0.0020
0.0015
0.0010
0.0005
0.0000
SPHK1
SPHK2
WT
sphk1-1
sphk2-1
D
Relative level of gene expression
0.14
0.12
0.10
0.08
0.06
0.04
0.01
0.00
0 min
5 min
10 min
20 min
40 min
ABI1
SPHK1
SPHK2

Figure 1

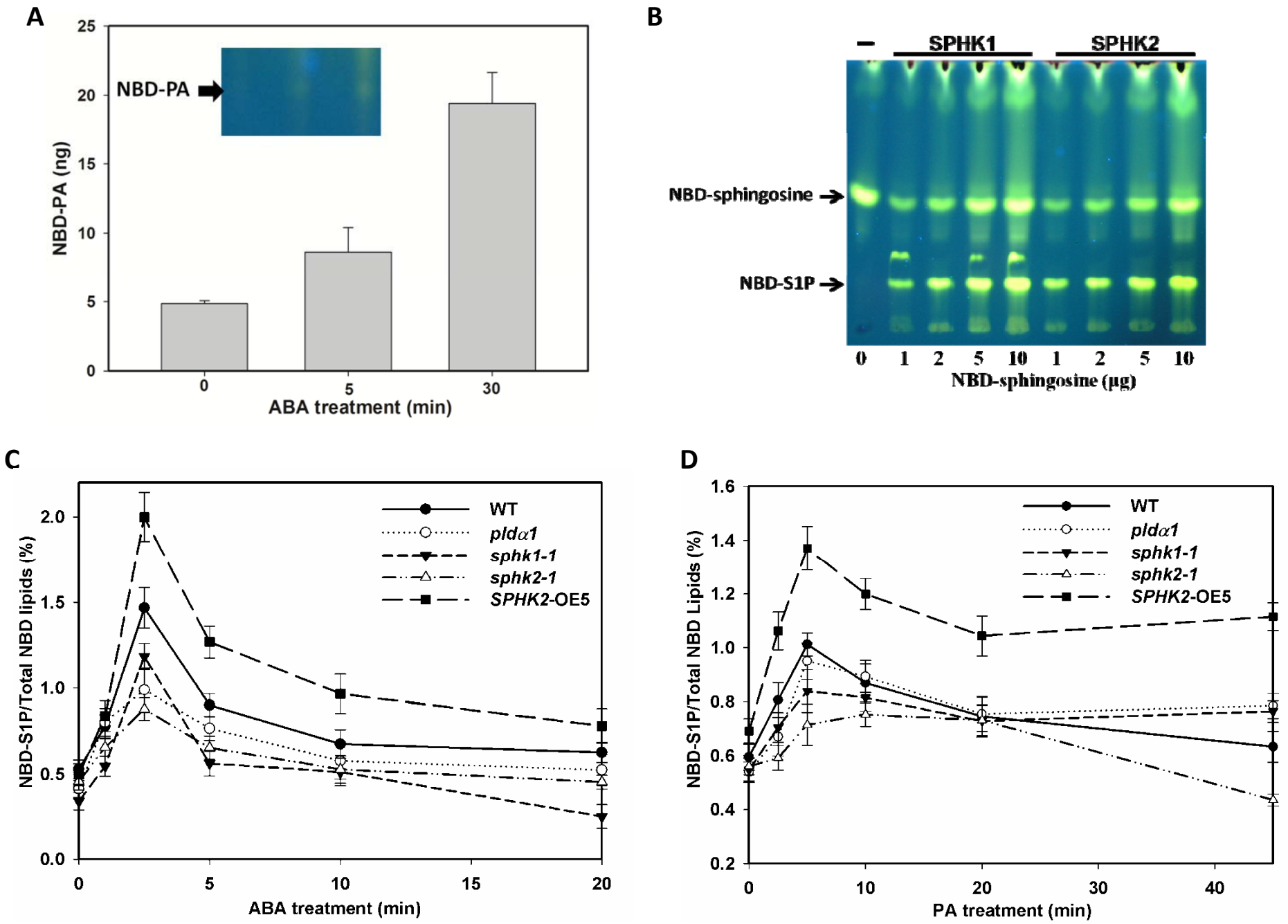
A
NBD-PA
NBD-PA (ng)
ABA treatment (min)
B
SPHK1
SPHK2
NBD-sphingosine
NBD-S1P
NBD-sphingosine (μg)
C
WT
pldα1
sphk1-1
sphk2-1
SPHK2-OE5
NBD-S1P/Total NBD lipids (%)
ABA treatment (min)
D
NBD-S1P/Total NBD Lipids (%)
PA treatment (min)

Figure 2

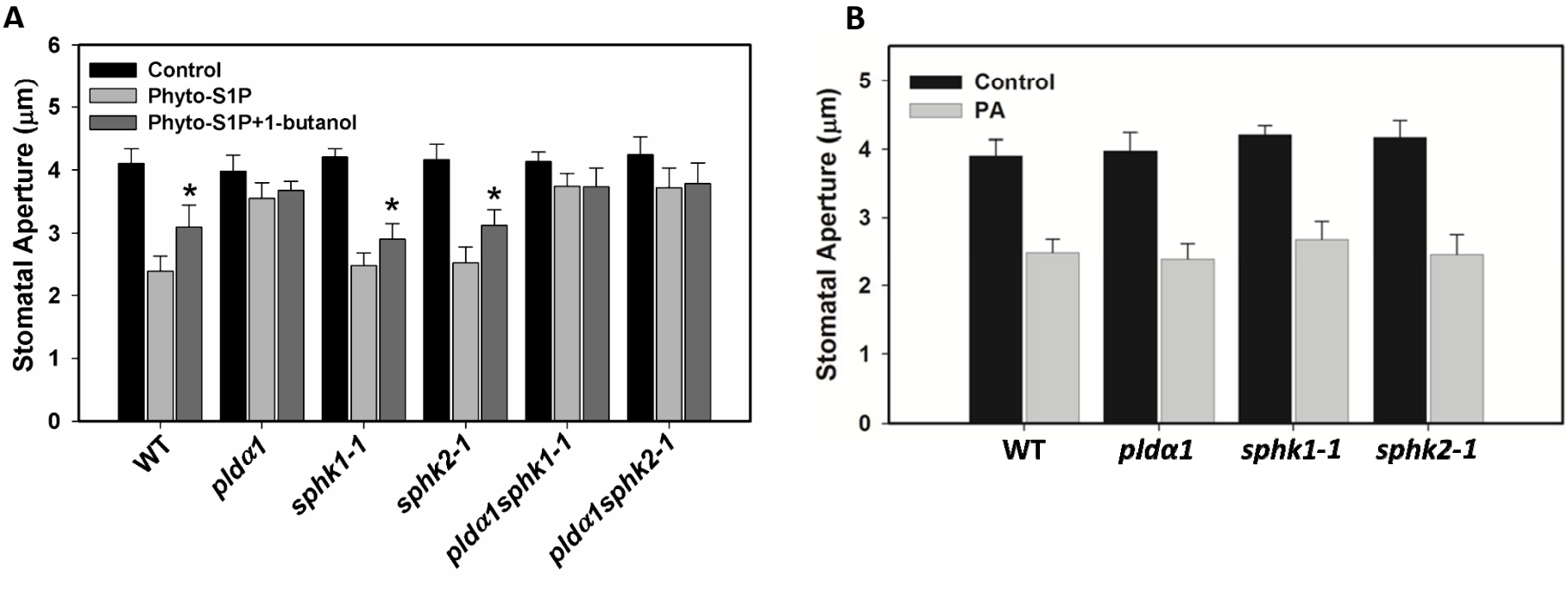
A
Stomatal Aperture (μm)
Control
Phyto-S1P
Phyto-S1P+1-butanol
*
*
*
WT
pldα1
sphk1-1
sphk2-1
pldα1sphk1-1
pldα1sphk2-1
B
Stomatal Aperture (μm)
Control
PA
WT
pldα1
sphk1-1
sphk2-1

Figure 3

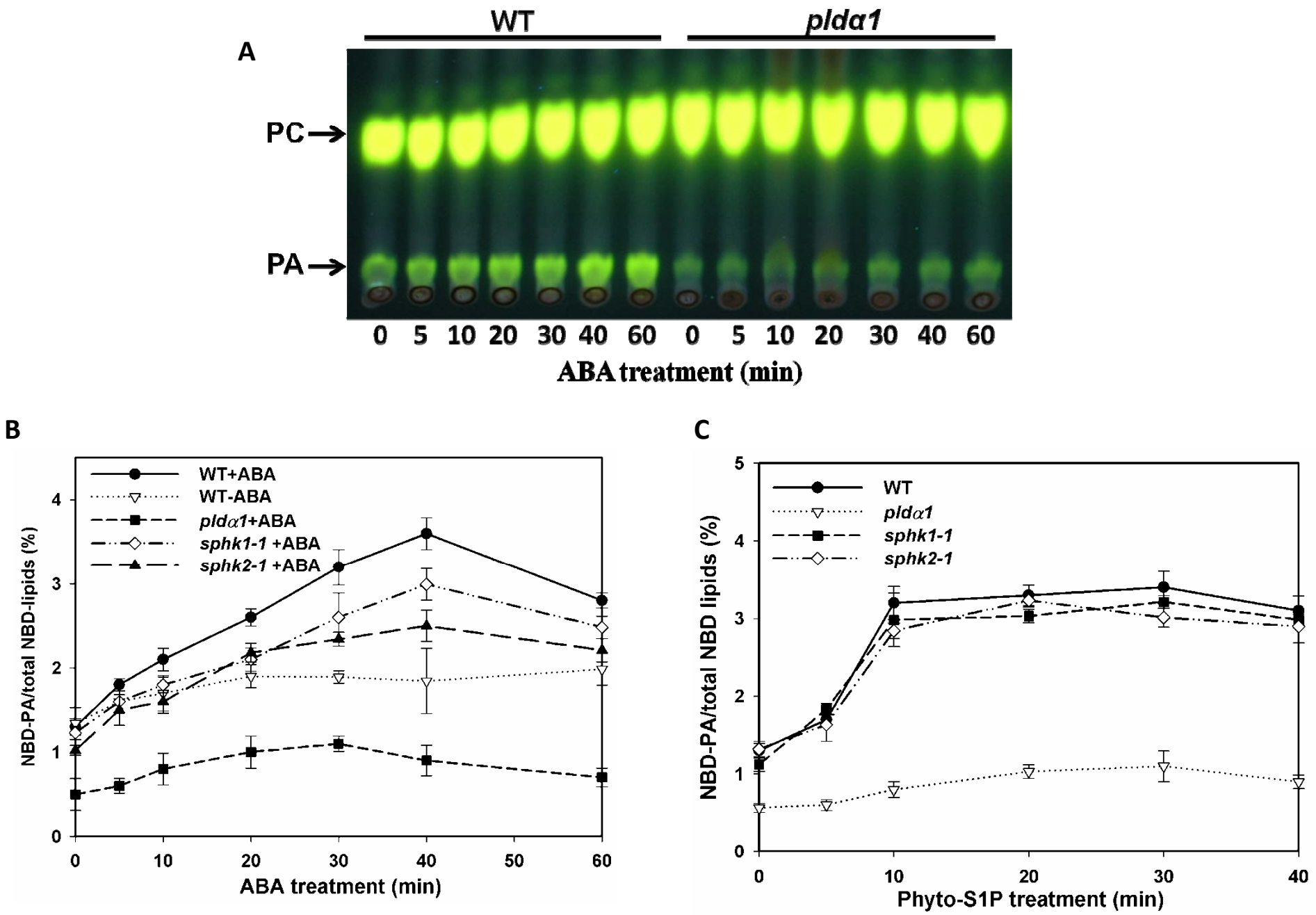
A
WT
pldα1
PC
PA
0 5 10 20 30 40 60 0 5 10 20 30 40 60
ABA treatment (min)
B
WT+ABA
WT-ABA
pldα1+ABA
sphk1-1 +ABA
sphk2-1 +ABA
NBD-PA/total NBD-lipids (%)
ABA treatment (min)
C
WT
pldα1
sphk1-1
sphk2-1
NBD-PA/total NBD lipids (%)
Phyto-S1P treatment (min)

Figure 4

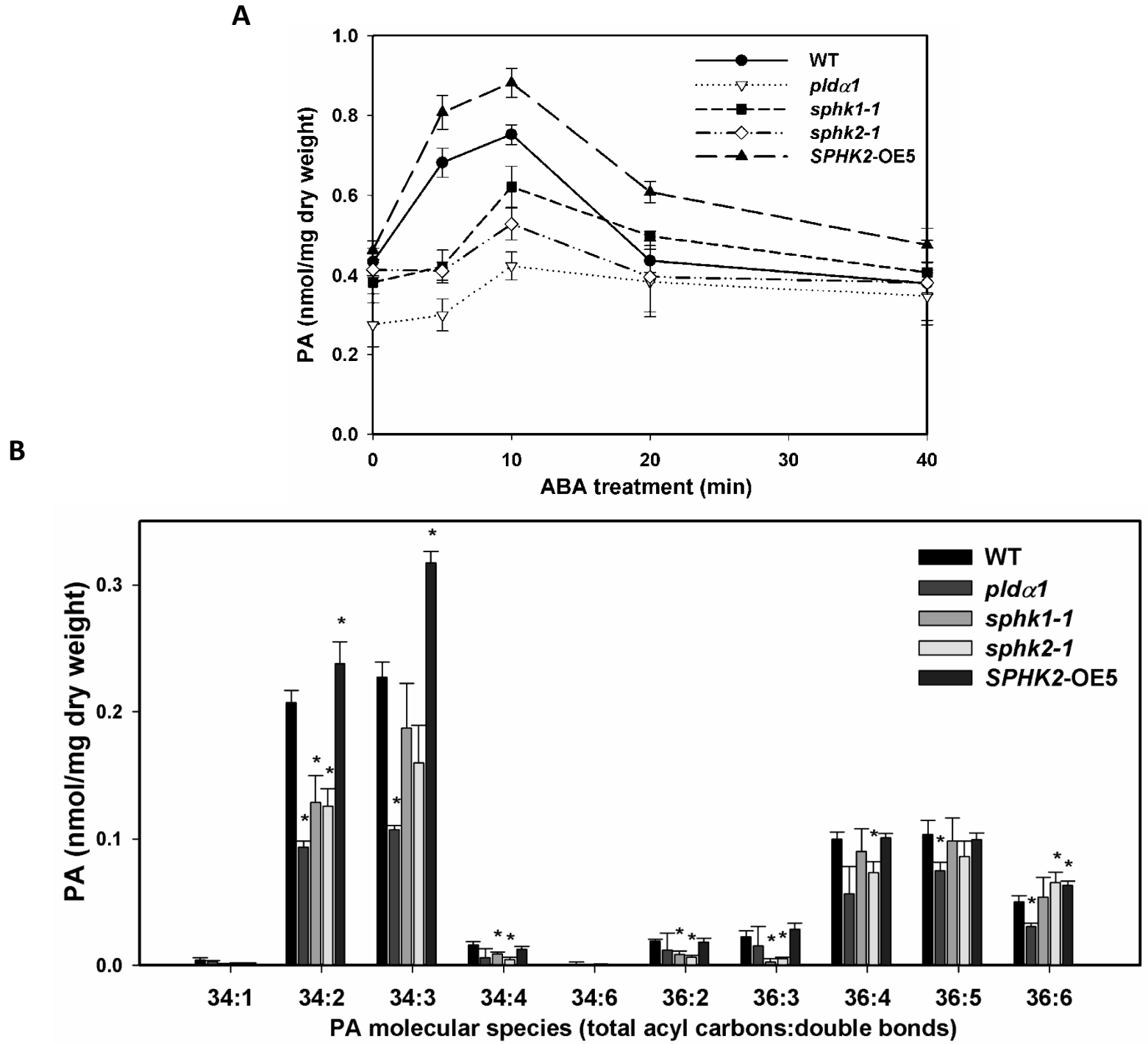
A
1.0
0.8
0.6
0.4
0.2
0.0
PA (nmol/mg dry weight)
0
10
20
30
40
ABA treatment (min)
WT
pldα1
sphk1-1
sphk2-1
SPHK2-OE5
B
0.3
0.2
0.1
0.0
PA (nmol/mg dry weight)
34:1
34:2
34:3
34:4
34:6
36:2
36:3
36:4
36:5
36:6
PA molecular species (total acyl carbons:double bonds)
WT
pldα1
sphk1-1
sphk2-1
SPHK2-OE5

Figure 5

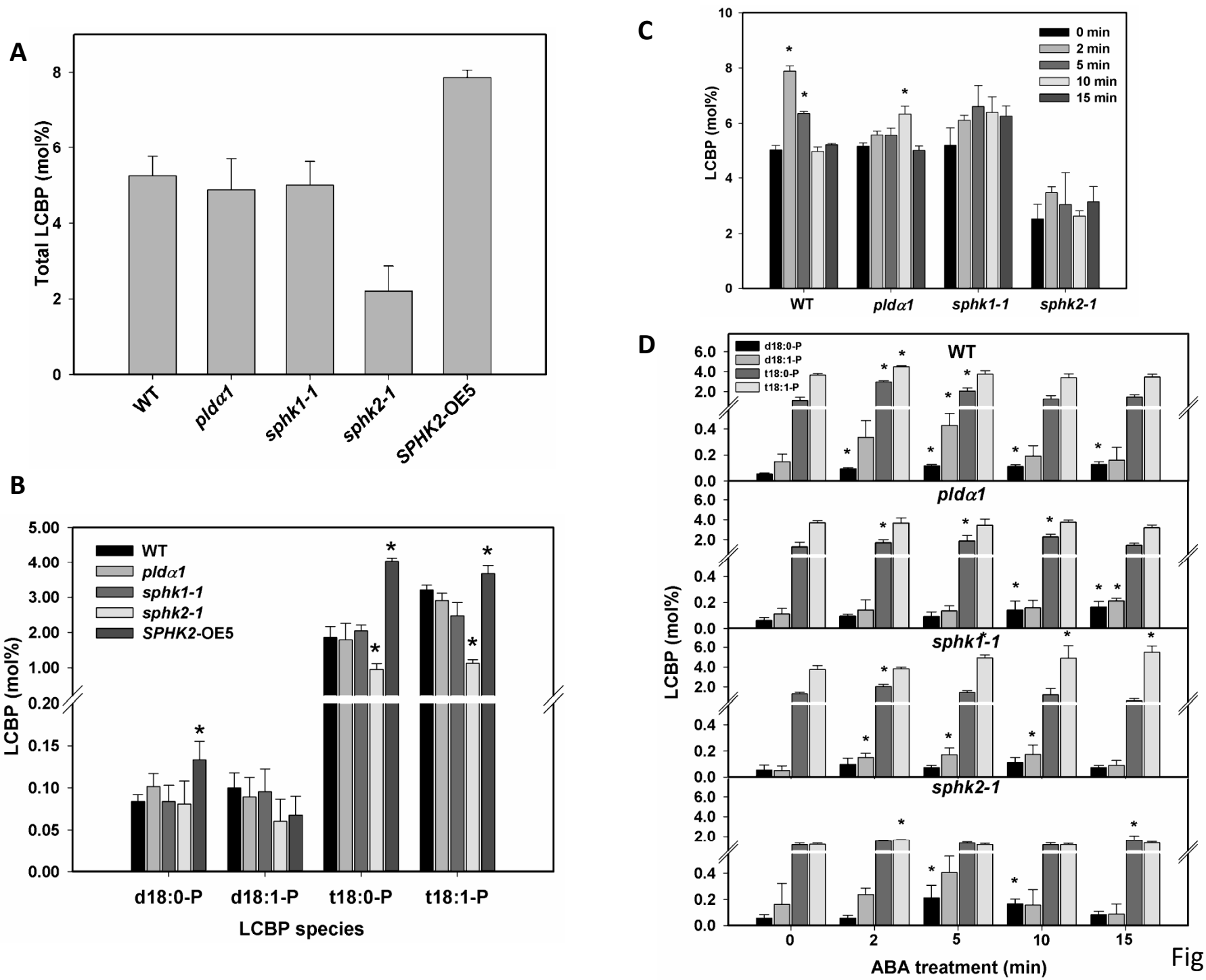
A
Total LCBP (mol%)
WT
pldα1
sphk1-1
sphk2-1
SPHK2-OE5
B
LCBP (mol%)
WT
pldα1
sphk1-1
sphk2-1
SPHK2-OE5
d18:0-P
d18:1-P
t18:0-P
t18:1-P
LCBP species
C
LCBP (mol%)
0 min
2 min
5 min
10 min
15 min
WT
pldα1
sphk1-1
sphk2-1
D
LCBP (mol%)
d18:0-P
d18:1-P
t18:0-P
t18:1-P
WT
pldα1
sphk1-1
sphk2-1
ABA treatment (min)

Figure 6

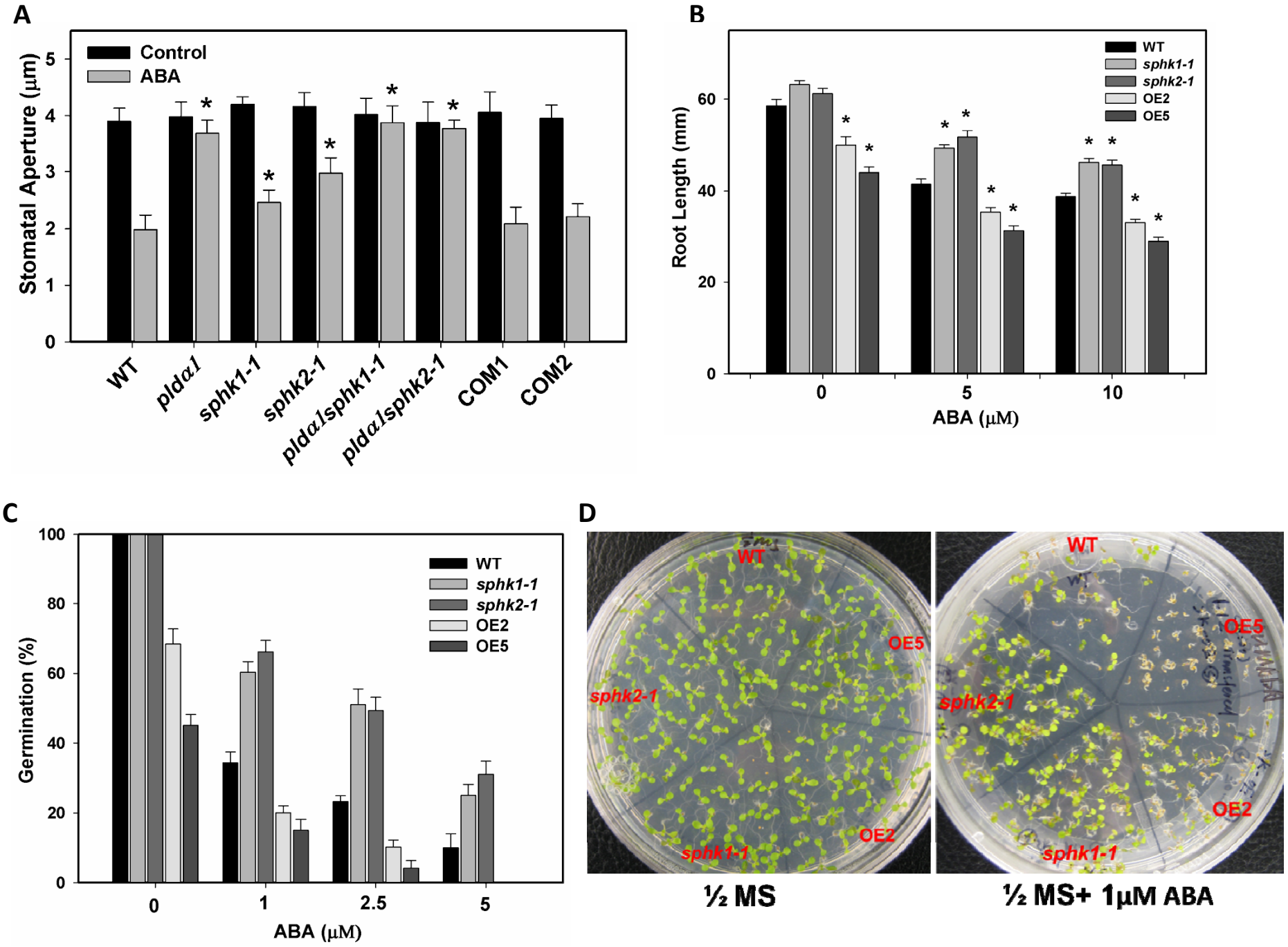
A
Control
ABA
Stomatal Aperture (μm)
WT
pldα1
sphk1-1
sphk2-1
pldα1sphk1-1
pldα1sphk2-1
COM1
COM2
B
WT
sphk1-1
sphk2-1
OE2
OE5
Root Length (mm)
ABA (μM)
C
Germination (%)
ABA (μM)
D
WT
OE5
sphk2-1
OE2
sphk1-1
½ MS
½ MS+ 1μM ABA

Figure 7

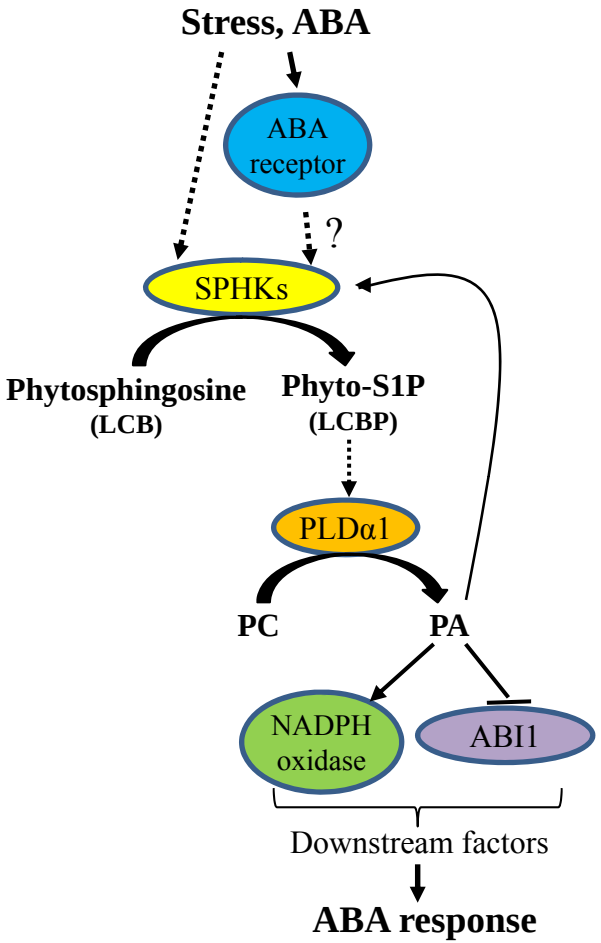
Stress, ABA
ABA receptor
?
SPHKs
Phytosphingosine (LCB)
Phyto-S1P (LCBP)
PLDα1
PC
PA
NADPH oxidase
ABI1
Downstream factors
ABA response

Figure 8

Supplemental Figures:

Supplemental Figure 1. Assay of SPHK activity using NBD-sphinogosine. Representative TLC image of SPHK activity using NBD-sphingosine-labeled protoplasts treated with 50 μM ABA for different times in WT, *pldα1,* and *sphk1-1*.

Supplemental Figure 2. PLDα1 activity assay with addition of phyto-S1P. *A*, TLC image of PLDα1 activity assay. PLDα1 activity assay was done using total protein extracted from WT and *pldα1 Arabidopsis* leaves. 2.5 μg total protein was incubated with 20 μg NBD-PC as substrate under PLDα1 reaction condition (25 mM Ca^{2+}, 100 mM MES, PH 6.0, 0.5 mM SDS). The assay was incubated at 30°C with shaking for 20 min. Knockout of PLD α1 resulted in more than 95% decrease of PA production, indicating PLDα1 is responsible for the PLD activity under this assay condition. PLDα1 activity was determined with addition of 5 μM or 25 μM phyto-S1P. There were three replicates for each condition. *B*, quantification of lipids isolated from sFigure 2A. The level of PA was calculated as the percentage of NBD-PA over the total NBD-labeled lipids. Values are means ± SE (n=3).

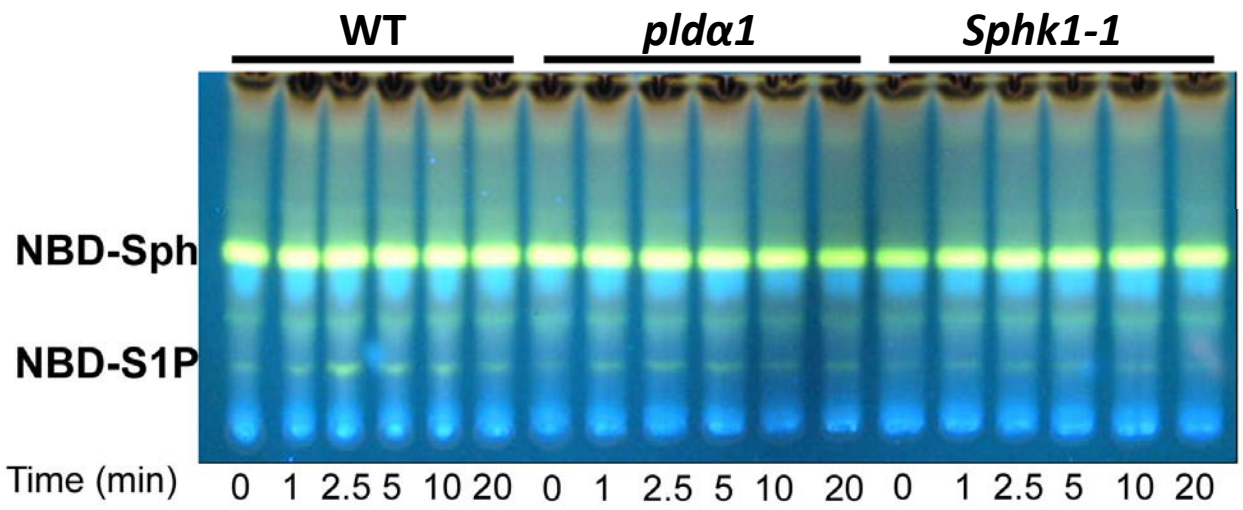

Supplemental 1

A

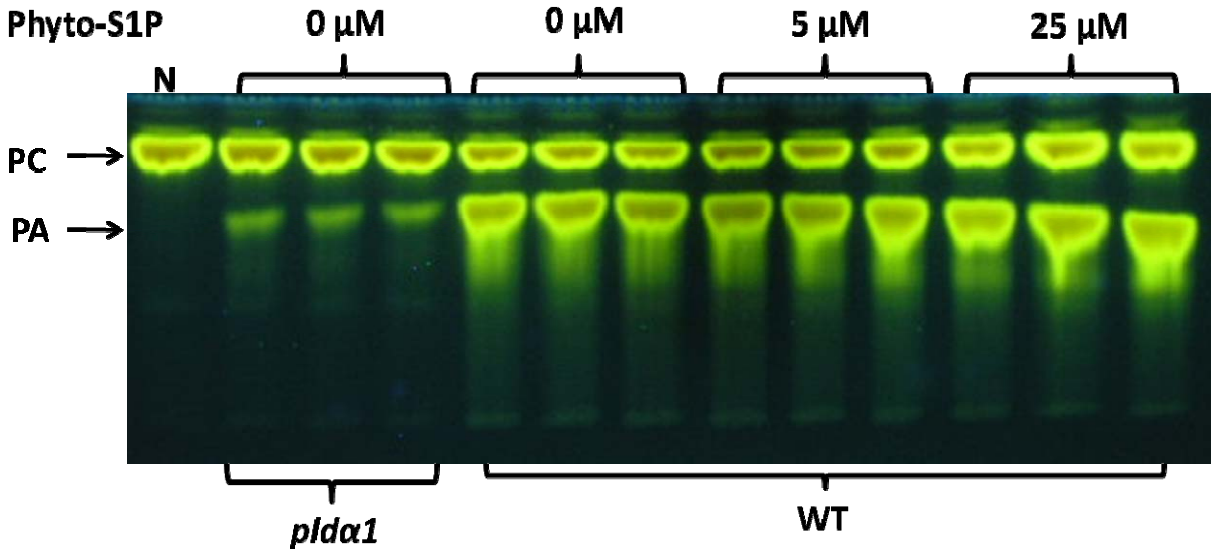

B

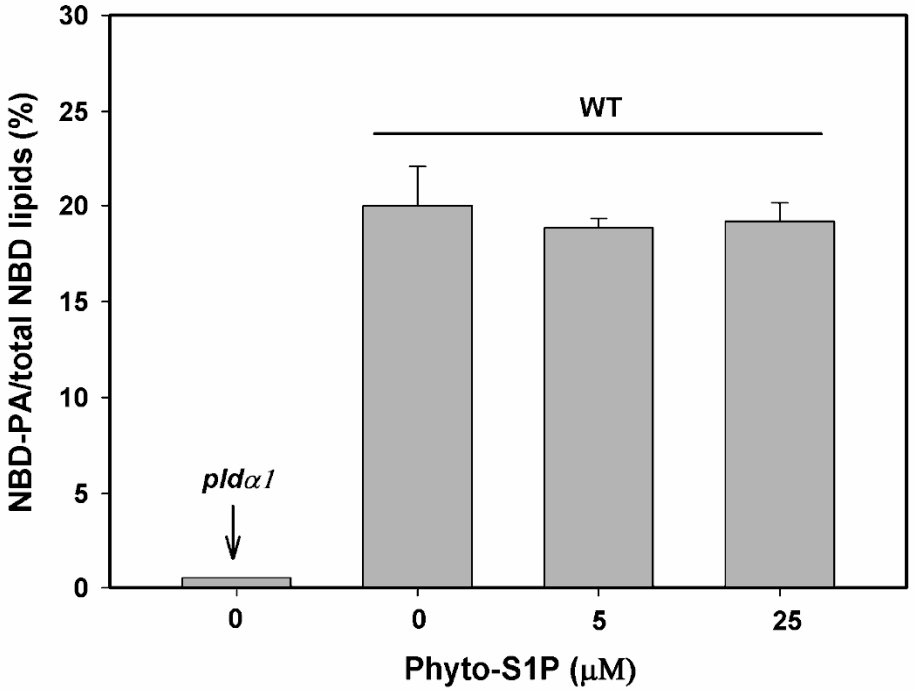

Supplemental 2